

Ab Initio Calculations of the Trigonal and Zero-Field Splittings in Trischelated Diketonato Complexes of Trivalent Chromium

Carl Ribbing, Kristine Pierloot, and Arnout Ceulemans*

Division of Quantum Chemistry, University of Leuven, Celestijnenlaan 200F, B-3001 Leuven, Belgium

Received February 12, 1998

The ground and excited states of the neutral tris(1,3-propanedionato)chromium(III) d^3 complex are investigated with quantum chemical methods. Trigonal splittings are calculated and compared with experiment for the first two excited quartet states ${}^4T_{2g}$ and ${}^4T_{1g}$. The effect of spin-orbit coupling is also introduced, and a reassignment is proposed for three absorption bands in the doublet region. Trigonal symmetry-induced mixing between the e_g and t_{2g} shells is found to be responsible for the unusually large zero-field splitting of the ${}^4T_{2g}$ ground state. Orbitals pictures are presented which illustrate the role of the phase-coupling effect from the unsaturated ligands.

1. Introduction

The tris(acetylacetonato)chromium(III) complex, $\text{Cr}(\text{acac})_3$, has been the subject of numerous spectroscopic, magneto-optical, and theoretical studies.¹ Especially the π -bonding role of the conjugated bidentate chain and the possible occurrence of a phase-coupling effect have attracted attention.²

On the basis of a detailed analysis in the framework of the angular overlap model (AOM) Atanasov et al. concluded that the trigonal splitting of the first spin-allowed band, ${}^4T_{2g} \leftarrow {}^4A_{2g}$, by some 800 cm^{-1} was indeed due to the phase-coupling effect.³ In a further study⁴ it was argued that the unusually large zero-field splitting (ZFS) of the ground state⁵ by 1.2 cm^{-1} could only be explained by assuming an anisotropic spin-orbit coupling mechanism. The low-temperature emission spectrum was assigned to phosphorescence from the $2\bar{A}({}^3/2)$ spin-orbit component of a trigonal 2E state with predominant 2E_g octahedral parentage.^{1,4} The extremely large ZFS⁶ and unusual g tensor^{7,8} of the doublet state remained poorly understood.

Progress in correlated methods of computational chemistry currently allows us to perform electronic structure calculations that can throw a new light on these issues. In this paper we report the first investigation of a trischelated Cr(III) complex with the unsubstituted 1,3-propanedionato ligand, PDO^- , using the complete active space methods CASSCF and CASPT2. The conclusions corroborate the results by Atanasov et al. concerning the phase-coupling origin of the trigonal splitting.^{3,4} In addition a new assignment for the doublet bands is suggested.

2. Computational Details

The calculations were performed with the MOLCAS program system,⁹ and the effective symmetry was limited to the C_2 subgroup of the actual D_3 point group. Optimized orbitals were obtained with the CASSCF method for each state. The active space was restricted to the five d orbitals. It was noticed during optimization that the orbitals acquired some ligand character, but only to a minor extent. Orbitals of e, a_1 , and a_2 type were prevented from mixing by using the supersymmetry option in the CASSCF program.

To introduce further correlation into the calculations a CASPT2^{9,10} calculation was performed for each state, using the CASSCF wave function as reference. In the CASPT2 calculations all electrons, except 1s, 2s, and 2p on chromium and 1s on carbon and oxygen, were correlated (95 electrons). ANO type basis sets¹¹ were chosen as follows: Cr(17s12p9d4f/6s4p3d1f), O(10s6p/3s2p), C(10s6p/3s2p), and H(7s/2s).

The geometry of the $\text{Cr}(\text{PDO})_3$ complex was determined in the following way. First we optimized the free PDO^- ligand with the constraint that the O–O distance is 2.77 \AA (see below). This produced a flat C_{2v} geometry for the PDO^- ligand. If the numbering of the carbons along PDO is O–C₁–C₂–C₃–O, the geometry is the following: distances (\AA), O–O = 2.77, O–C₁ = 1.33, C₁–C₂ = 1.39, C₁–H₁ = 1.10, C₂–H₂ = 1.08; angles (deg), O–C₁–C₂ = 124.6, O–C₁–H₁ = 119.1, C₁–C₂–H₂ = 117.8. If the PDO^- ligands are placed around the Cr^{3+} ion so that the oxygens are in exact octahedral positions, an O–O distance of 2.77 \AA corresponds to a Cr–O distance of $2.77/\sqrt{2} = 1.96\text{ \AA}$. For the closely related $\text{Ga}(\text{acac})_3$ and $\text{Cr}(\text{acac})_3$ complexes the geometry is available from X-ray diffraction data^{12–14} and the coordination of the oxygens is very close to

(1) Schönherr, T. *Top. Curr. Chem.* **1997**, *191*, 87.

(2) Ceulemans, A.; Vanquickenborne, L. G. *Pure Appl. Chem.* **1990**, *62*, 1081.

(3) Atanasov, M. A.; Schönherr, T.; Schmidtke, H. H. *Theor. Chim. Acta* **1987**, *71*, 59.

(4) Atanasov, M.; Schönherr, T. *Inorg. Chem.* **1990**, *29*, 4545.

(5) Elbers, G.; Remme, S.; Lehmann, G. *Inorg. Chem.* **1986**, *25*, 896.

(6) Schönherr, T.; Eyring, G.; Linder, R. *Z. Naturforsch.* **1983**, *38*, 736.

(7) Fields, R. A.; Haindl, E.; Winscom, C. J.; Khan, Z. H.; Plato, M.; Möbius, K. *J. Chem. Phys.* **1984**, *80*, 3082.

(8) Fields, R. A.; Winscom, C. J.; Haindl, E.; Plato, M.; Möbius, K. *Chem. Phys. Lett.* **1986**, *124*, 121.

(9) Andersson, K.; Fülscher, M. P.; Karlström, G.; Lindh, R.; Malmqvist, P.-Å.; Olsen, J.; Roos, B. O.; Sadlej, A. J.; Blomberg, M. R. A.; Siegbahn, P. E. M.; Kellö, V.; Noga, J.; Urban, M.; Widmark, P.-O. *MOLCAS*, Version 3; Department of Theoretical Chemistry: Chemistry Center, University of Lund, P.O.B. 124, S-221 00 Lund, Sweden, 1994.

(10) Andersson, K.; Malmqvist, P.-Å.; Roos, B. O.; Sadlej, A. J.; Wolinski, K. *J. Phys. Chem.* **1990**, *94*, 5483.

(11) Pierloot, K.; Dumez, B.; Widmark, P.-O.; Roos, B. O. *Theor. Chim. Acta* **1995**, *90*, 87.

(12) Dymock, K.; Palenik, G. J. *Acta Crystallogr.* **1974**, *30*, 1364.

(13) Morosin, B. *Acta Crystallogr.* **1965**, *19*, 131.

octahedral with Cr–O distances corresponding to the above value. For the calculations on Cr(PDO)₃ we used a geometry of the complex with oxygens in exact octahedral positions and all Cr–O distances at 1.96 Å.

In addition to the above calculations we also performed spin–orbit coupling calculations. This was done with an effective one-electron spin–orbit operator, where a parameter, the effective charge, is scaled so as to reproduce experimental excitation energies of the free Cr(III) ion. The state optimized in the CASSCF and compared with the experimental spectrum, was the ⁴F state.¹⁵ Further the orbitals were averaged (via the one electron density matrix) to get degenerate p and d shells. In this way the value of the effective charge was determined to 12 in atomic units of charge and, the corresponding one-electron orbital coupling matrix element between the ionic d orbitals to $\xi = 285 \text{ cm}^{-1}$.

The spin–orbit couplings between the different states in the complex were calculated according to the following procedure.¹⁶ First, a set of orbitals was chosen from the CASSCF calculation of the ²A₂ state. These orbitals have the correct degeneracy and symmetry of the D₃ group. With these orbitals a configuration interaction (CI) calculation is then performed and the CI eigenvectors corresponding to different roots are saved. The Slater determinants were generated according to the restricted active space CI method. We constructed three different orbital subspaces, one with doubly occupied orbitals from which single and double excitations are performed, a second (active) space in which any number of excitations is allowed, and a third (virtual) space in which zero, one, or two electrons can be promoted from the other subspaces.

Next, the CI eigenvectors were used to calculate all spin–orbit couplings. According to the Wigner–Eckart theorem¹⁷ we only need to calculate CI eigenvectors from the $M_s = 1/2$ space. In this space components of both $S = 1/2$ and $=3/2$ are included. With the 3J coupling coefficients we can generate all the other components with $M_s = -3/2, -1/2, 1/2, 3/2$. For this purpose we decompose the spin–orbit operator into components with symmetry adaption to the rotational group

$$\hat{H}_{\text{so}} = 1/\sqrt{2}[i T_y^1 - T_x^1 + i T_y^{-1} + T_x^{-1}] + T_z^0$$

The spin–orbit tensor operators T_a^m are defined as sums over one-electron operators: $a = \{x, y, z\}$, $m = \{1, 0, -1\}$, $s^+ = (s^x + i s^y)$, $s^- = (s^x - i s^y)$:

$$T_a^m = C(m) \frac{\alpha^2}{2} \sum_i \frac{Z_{\text{eff}}}{\hat{r}^3} \hat{l}_i^a \hat{s}_i^m$$

$$s_i^m = \{s_i^+, s_i^z, s_i^-\}$$

$$C(m) = \left\{ -\frac{1}{\sqrt{2}}, 1, \frac{1}{\sqrt{2}} \right\}$$

The Cartesian coordinate orbital operator, $Z_{\text{eff}} \hat{r}^{-3} \hat{l}_i^a$, is computed, including the \hat{r}^{-3} operator centered on Cr(III), over the atomic orbital basis set and later transformed to molecular orbital

basis; since we have a one-center approximation, only the projections of the d type orbitals centered on Cr(III) are included.

It can be verified that the operators T_a^m form a basis for the irreducible representation of order 1 of the rotational group R(3),¹⁸ it is the case if

$$[S_z, T_a^m] = m T_a^m, \quad [S_{\pm}, T_a^m] = \sqrt{2 - m(m \pm 1)} T_a^{m \pm 1}$$

Below we check one of the commutators, $[S_+, T_a^0]$, where $S_+ = \sum_i s_i^+$

$$\begin{aligned} S_+ T_a^0 - T_a^0 S_+ &= Z_{\text{eff}} \sum_{ij} (s_i^+ s_j^z - s_j^z s_i^+) \hat{l}_{ij}^a \hat{r}^{-3} \\ &= Z_{\text{eff}} \sum_i -s_i^+ \hat{l}_i^a \hat{r}^{-3} = \sqrt{2} T_a^1 \end{aligned}$$

where we assumed that the products of the one-electron spin-operators commute if $i \neq j$. Since the transformation properties of the spin–orbit operators T_a^m are irreducible, the Wigner–Eckart theorem can be used to achieve a relation between the matrix elements and a quantity known as the reduced matrix element.^{17,18} The general expression for matrix elements in a basis (sums of Slater determinants) that are eigenfunctions to S^2 and S_z is

$$\begin{aligned} \langle S, M_s, E | T_a^m | S', M_s', E' \rangle &= \\ &= (-1)^{(S-M_s)} \begin{pmatrix} S & 1 & S' \\ -M_s & m & M_s' \end{pmatrix} \langle S, E || T_a || S', E' \rangle \end{aligned}$$

where $\langle S, E || T_a || S', E' \rangle$ is the reduced matrix element without any dependence of the M_s . The matrix elements expressed in this form greatly simplify the calculations since the spin symmetry can be separated out from the problem and is contained in the 3J symbol.

We calculated only the matrix elements in the $M_s = 1/2$ space with the spin–orbit operator T_a^0 , $\langle S, 1/2, E | T_a^0 | S', 1/2, E' \rangle$ and the related reduced matrix elements, $\langle S, E || T_a || S', E' \rangle$, from the Wigner–Eckart theorem. From the reduced matrix elements the Hermitian spin–orbit matrix is formed; with dimension equal to the total number of spin states, counting all different M_s components. Since the spin–orbit operator is entirely complex (the angular momentum operator, l) and the CI basis real, the diagonal elements of the spin–orbit coupling are zero. Thus the diagonal elements in the Hermitian spin–orbit matrix are the real excitation energies for each state from the above CI calculation.

Finally, diagonalization of the above spin–orbit matrix gives spin–orbit coupled double group states. In the D₃ double group, spin–orbit coupled states for an odd number of electrons can be classified according to the symmetry species $2\bar{A}^{(3/2)}$ or $E^{(1/2)}$. The ³/₂ and ¹/₂ denote the projection of the coupled angular momentum along the trigonal axis. For an odd number of electrons in absence of external magnetic field there will always be a degeneracy of at least two (Kramers degeneracy). The last step directly gives the spin–orbit splittings of the different states. In this step it is also possible to make use of the calculated CASPT2 energies to improve upon the correlation treatment in the spin–orbit coupling calculation. The diagonal values of the spin–orbit coupling matrix can be substituted with the more accurate CASPT2 energies before diagonalization. This

- (14) Schönherr, T.; Atanasov, M. A.; Schmidtke, H. H. *Inorg. Chem. Acta* **1988**, *141*, 27.
 (15) Moore, C. E. *Atomic Energy Levels*; Circular of the National Bureau of Standards 467; National Bureau of Standards: Washington, DC, 1952.
 (16) Ribbing, C.; Daniel, C. J. *Chem. Phys.* **1994**, *100*, 6591.
 (17) Weissbluth, M. *Atoms and Molecules*; Academic Press: London, 1978.

- (18) Chisholm, C. D. H. *Group Theoretical Techniques in Quantum Chemistry*; Academic Press: London, 1976.

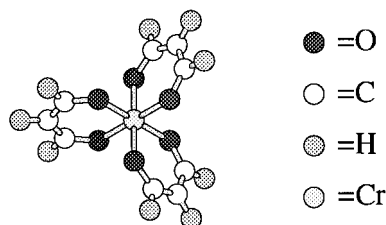


Figure 1. Geometry of the $\text{Cr}(\text{PDO})_3$ complex viewed from the trigonal axis.

is justified by noting that the remaining correlation correction (going from the restricted full CI to the CASPT2) will not change the wavefunction to a large extent; only the diagonal elements will change.

In the calculations of the spin-orbit coupling we used a restricted full CI expansion of about half a million determinants in each symmetry and $M_s = 1/2$. We included double excitations from the three highest occupied orbitals of ligand character, full CI of the 3d orbitals, and single and double excitations to 26 of the lowest virtual orbitals. The results without spin-orbit coupling of the CI calculation are presented in Figure 2 together with the CASSCF, CASPT2, and experimental values for $\text{Cr}(\text{acac})_3$. The calculated spin-orbit levels originating from the lower doublet states are listed in Table 1. We have also included the improved (CASPT2 substitution) spin-orbit calculation.

3. Results

Fatta and Lintved¹⁹ have measured the excitation energies for a number of different trischelated 1,3-diketonato Cr(III) compounds in solution. The effect of the solvent was rather small. The excitation energies for the lowest ${}^2E_g \leftarrow {}^4A_{2g}$ and ${}^4T_{2g} \leftarrow {}^4A_{2g}$ states show little variation in the series of diketonato complexes, with deviations from average not exceeding 250 cm^{-1} . In contrast, for the second spin-allowed band of ${}^4T_{1g} \leftarrow {}^4A_{2g}$ character and for the first ligand-to-metal charge transfer (LMCT) transition there are larger variations. Obviously the charge transfer is strongly affected by the substituents on the diketonato ligands. The ${}^4T_{1g} \leftarrow {}^4A_{2g}$ excitation is in most spectra obtained as a shoulder and it is probable that the variation is due to imprecise measurements; also interactions with the close lying LMCT state could add to this variation.

More precise measurements of the fine structure of some of the d-d transitions in the diketonato complexes have been made for $\text{Cr}(\text{acac})_3$ doped into the host material $\text{Al}(\text{acac})_3$.^{3,4,7} Here both absorption and emission spectra have been measured in different polarizations. Of special interest are the trigonal splittings of the ${}^4T_{2g}$ and ${}^4T_{1g}$ states. For the lower ${}^4T_{2g}$ state the experimental splitting amounts to 800 cm^{-1} , with the 4A_1 component below the 4E component. However for ${}^4T_{1g}$ the splitting is not observable due to the overlap with the intense LMCT absorption. Since the lowest excitation energies of ${}^2E_g \leftarrow {}^4A_{2g}$ and ${}^4T_{2g} \leftarrow {}^4A_{2g}$ are not much affected in going from 2,4-pentanedionate (acac) to 1,3-propanedionate (PDO) as ligand, it is likely that a relevant comparison can also be made between the calculated splitting for $\text{Cr}(\text{PDO})_3$ and the experimental splitting for $\text{Cr}(\text{acac})_3$.

We now turn to the results of the calculations. Figure 2 shows the calculated excitation energies at both the CASSCF and the CASPT2 level for the $\text{Cr}(\text{PDO})_3$ compound. We have also included the experimental energies of the doped complex in $\text{Al}(\text{acac})_3$ lattice. Going from CASSCF to CASPT2 the average

of the quartet states is not much affected. However, the splittings of the 4T states, and especially of the lower ${}^4T_{2g}$ state, increase considerably. We will return to this below. The position of the doublet states is also strongly affected by correlation. The difference between the calculated CASPT2 excitation energy for the lowest doublet state, and the measured phosphorescent level, is larger than for the lowest quartet state. The same observation has already been made in theoretical calculations of spectra of other Cr(III) compounds like CrF_6^{3-} and $\text{Cr}(\text{CN})_6^{3-}$.²⁰⁻²²

The trigonal splittings of the octahedral 4T states are seen to increase at the CASPT2 level. The increase is somewhat larger for the ${}^4T_{2g}$ state than for the ${}^4T_{1g}$ state. The former state is split with 4A_1 below 4E . The CASPT2 calculations yield a splitting of 1300 versus 800 cm^{-1} experimentally.³ Both the absolute excitation energies and the trigonal splitting of these states compare well with experiment. For the next excited quartet state ${}^4T_{1g}$ an inverse splitting is calculated, with 4E now below 4A_2 ; the magnitude is 1000 cm^{-1} . The absolute position of this state shows larger deviation from the measured position both for $\text{Cr}(\text{acac})_3$ and $\text{Cr}(\text{PDO})_3$.¹⁹ This fact may be due to interaction with the lowest charge transfer state. Experimentally both for acac and PDO as ligand the charge transfer is at about 26 000 cm^{-1} , in near coincidence with the ligand field ${}^4T_{1g}$ state. The splitting of the second quartet band has not been determined in the absorption spectrum of $\text{Cr}(\text{acac})_3$, since only the 4E component could be observed.³ Our calculations determine the 4A_2 component to be higher in energy, thus probably hidden in the charge-transfer band. In any case this transition is bound to be very weak since it is dipole forbidden.

Next we will discuss the spin-orbit coupling calculations. In Table 1 we present the calculated energies after spin-orbit coupling. Experimentally the 4A_2 ground state has a rather large ZFS of 1.2 cm^{-1} with $2\bar{A}({}^3/2)$ below $E(1/2)$.^{1,7} A simple ligand field analysis^{2,23,24} reveals that this splitting cannot arise from isotropic interaction with the lowest quartet state through second-order perturbation—the trigonal splitting of the quartet state would have to be some 10 000 cm^{-1} in order to induce a 1.2 cm^{-1} ZFS of the ground state. However, it has been noted that a possible mechanism to induce large ZFS is configuration interaction within the d shell, with perturbation loops running over the trigonal ligand field.^{24,25}

Our spin-orbit coupled CI calculation of the spin-orbit splitting of the ground state gives the values: 1.0 cm^{-1} at the CI level and 1.2 cm^{-1} with CASPT2 diagonal correction. The splitting is of the correct sign with $2\bar{A}({}^3/2)$ below $E(1/2)$, and in good agreement with experiment. The agreement with CASPT2 correction is a bit fortuitous since the lower doublet states are still off by a few thousand wavenumbers and further lowering would increase the ZFS. The ground state splitting seems to arise mainly from interaction of the ground state with the trigonal components of the ${}^4T_{2g}$ state and of the higher ${}^2T_{2g}$ state; they both contribute approximately to the same extent. The ZFS originates entirely from anisotropic spin-orbit coupling matrix elements with the excited states, the trigonal splitting of the excited states being unimportant (this was tested

(19) Fatta, A. M.; Lintved, R. L. *Inorg. Chem.* **1971**, *10*, 478.

(20) Seijo, L.; Barandiarán, Z.; Pettersson, L. G. M. *J. Chem. Phys.* **1993**, *98*, 4041.

(21) Pierloot, K.; Vanquickenborne, L. G. *J. Chem. Phys.* **1990**, *93*, 4154.

(22) Pierloot, K.; Van Praet, E.; Vanquickenborne, L. G. *J. Phys. Chem.* **1993**, *97*, 12220.

(23) Ballhausen, C. J. *Introduction to Ligand Field Theory*; McGraw-Hill: London, 1962.

(24) Macfarlane, R. M. *J. Chem. Phys.* **1967**, *47*, 2066.

(25) McGarvey, B. R. *J. Chem. Phys.* **1964**, *41*, 3743.

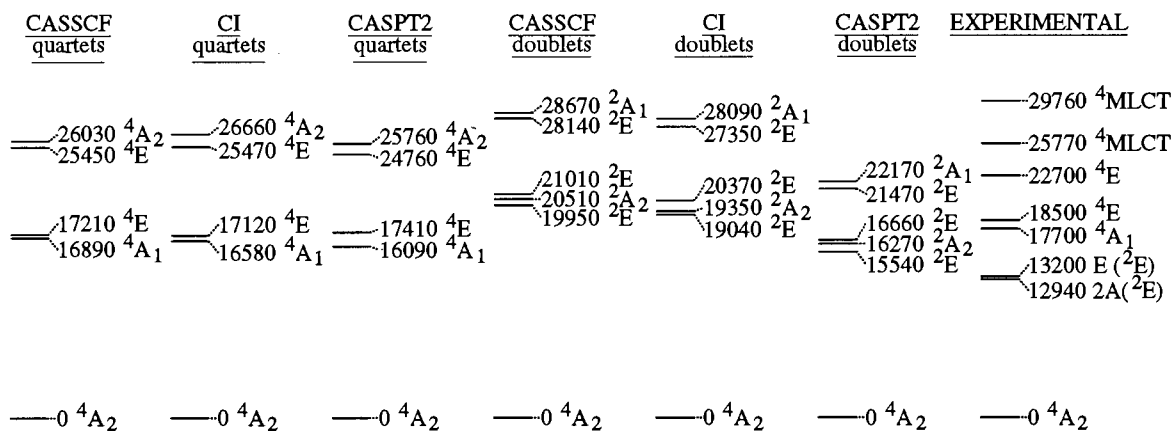


Figure 2. Calculated excitation energies for the quartet and doublet levels at three stages of calculation: CASSCF, CI, and CASPT2 (see text). For comparison experimental results from refs 3, 6, and 19.

Table 1. Calculated Energies of the Spin–Orbit States Belonging to Representations $E^{(1/2)}$ and $2\bar{A}^{(3/2)a}$

O_h	D_3	D_3 double group	CI		CASPT2 shifted	
			energies cm^{-1}	ZFS cm^{-1}	energies cm^{-1}	ZFS cm^{-1}
${}^2T_{1g}$	2E	$E^{(1/2)}$	20 420	110	16 672	75
		$2\bar{A}^{(3/2)}$	20 310		16 597	
2E_g	2A_2	$E^{(1/2)}$	19 358		16 321	
		2E	$E^{(1/2)}$	19 070 ^b	–12	15 476
${}^4A_{2g}$	4A_2	$2\bar{A}^{(3/2)}$	19 082		15 423 ^b	
		$E^{(1/2)}$	–9.9	1.0	–9.8	1.2
		$2\bar{A}^{(3/2)}$	–10.9		–11.0	

^a The pattern of splitting is given going from O_h to D_3 and further including spin–orbit coupling. Two calculations are presented: CI and a procedure where the diagonal elements corresponding to the lowest 2E , 2A_2 , 2E , 4A_1 , 2E , and 4A_2 of the spin–orbit matrix were shifted according to CASPT2 before diagonalization. This changes the lowest doublet state from $E^{(1/2)}$ to $2\bar{A}^{(3/2)}$. ^b Lowest doublet component.

by artificially removing the trigonal splitting of the ${}^4T_{2g}$ state). We will come back to this point in the discussion.

The lowest excited doublet states are ${}^2T_{1g}$ (2A_2 and 2E) and 2E_g (2E) with the latter lowest in energy. From absorption spectra, the ZFS of the lowest state in $\text{Cr}(\text{acac})_3$ has been estimated to amount to 220–290 cm^{-1} depending on the site in the host material.^{4,6} The results in Table 1 clearly indicate that such a large ZFS cannot be reproduced by the present calculations. The lower state of 2E_g parentage is split by only 53 cm^{-1} with $2\bar{A}^{(3/2)}$ below $E^{(1/2)}$ at CASPT2 level. For the higher 2E state of ${}^2T_{1g}$ parentage the calculated splitting amounts to 75 cm^{-1} , with $2\bar{A}^{(3/2)}$ below $E^{(1/2)}$. The parentages for these CASSCF wavefunctions could be assigned unambiguously from the principal determinants, which precisely match the trigonal combinations of reference 26. As we already noted, the energies of the lowest doublet states are substantially overestimated by the present calculations. To check if this discrepancy had any influence on the doublet ZFS we artificially lowered the doublet states. We shifted the diagonal elements of the 2E_g (2E) and ${}^2T_{1g}$ (${}^2E + {}^2A_2$) further down than CASPT2, so that the lowest 2E was at 13 000 cm^{-1} now well below the 4T states. The ZFS pattern did not change much; the ZFS of the lowest 2E state decreased while for the higher 2E it increased somewhat. There is a difference in the splitting pattern of the two 2E states: the higher 2E with ${}^2T_{1g}$ parentage, splits linearly with increasing

spin–orbit coupling while the lower has a quadratic dependence. This could be concluded from a series of calculations with increasing spin–orbit coupling, and it explains the change of sign of the ZFS for the lower 2E state that couples at second order with the lowest ${}^4T_{2g}$ state.

The lowest emitting state is believed to be of $2\bar{A}^{(3/2)}$ character,^{4,6} which coincides with the calculation with CASPT2 correction. On the basis of the calculated energy differences at the CASPT2 level and the spin–orbit splitting (see Figure 2 and Table 1), an alternative assignment may be suggested that would resolve the difficulty with the excited-state ZFS of the lowest 2E . In this alternative the three observed peaks at 12 940, 13 200, and 13 500 cm^{-1} are attributed to spin–orbit components of the 2E (2E_g), 2A_2 (${}^2T_{1g}$), and 2E (${}^2T_{1g}$) states, respectively. Remains however the difficulty to reconcile the 2E assignment of the emitting state with the experimentally observed excited state **g** tensor.^{7,8} Further investigation of this problem would require the ab initio calculation of the Zeeman effect.

4. Discussion

In this section we will be concerned with the origin of the trigonal splitting. The phase-coupling model^{2,27–29} relates the trigonal splitting of the t_{2g} shell in an orthoaxial trischelated complex to a difference in π -bonding between the in-phase and out-of-phase coupled ligand π -orbitals of the conjugated bidentates.

$$\Delta(t_{2g}) = E(e) - E(a_1) = \frac{3}{2}(e_\psi - e_\chi) \quad (1)$$

Here e_ψ and e_χ are bonding parameters for in-phase and out-of-phase interactions, respectively. From a spectral fit of the spin-allowed bands Atanasov et al.³ deduced a $\Delta(t_{2g})$ value of approximately +2100 cm^{-1} . According to simple MO arguments the positive sign of the splitting is explained by a dominating π -donor interaction from the ψ -type ligand HOMO ($e_\psi > 0$).^{2,28} Acceptor interactions with a χ -type ligand LUMO ($e_\chi < 0$) may further contribute to the splitting. In the present calculation these orbital pathways can indeed be recognized in MO plots. The orbitals that diagonalize the density matrix for the active space are not very informative in this respect, since they are of almost pure 3d character. On the other hand pictures of the ligand frontier orbitals clearly reveal metal–ligand

(26) Ceulemans, A. Orbital models and the photochemistry of transition-metal complexes. In *Vibronic Processes in Inorganic Chemistry*; Flint, C. D., Ed.; Kluwer Academic Publishers: Dordrecht, 1989; p 221.

(27) Ceulemans, A.; Bongaerts, N.; Vanquickenborne, L. G. *Inorg. Chem.* **1987**, *26*, 1566.

(28) Ceulemans, A.; Dendooven, M.; Vanquickenborne, L. G. *Inorg. Chem.* **1985**, *24*, 1159.

(29) Schäffer, C. E.; Yamatera, H. *Inorg. Chem.* **1991**, *30*, 2840.

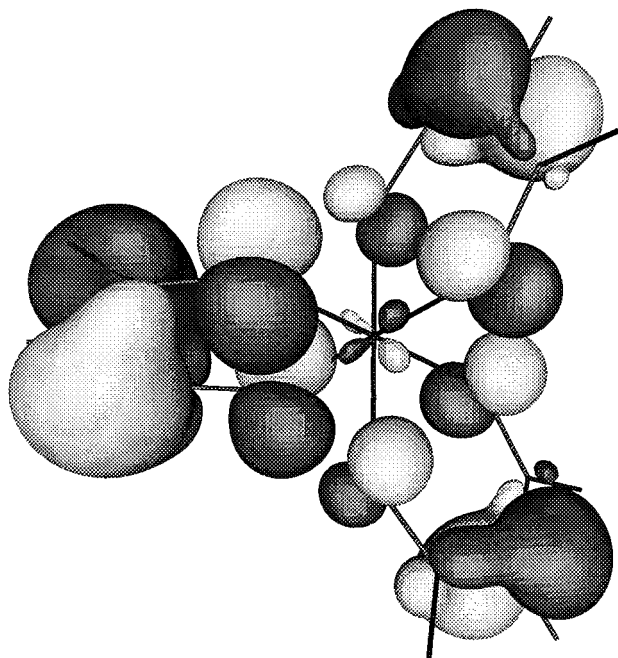


Figure 3. Contour plot of the highest occupied ligand ψ type orbital with e symmetry. Note delocalization over an $e(t_{2g})$ metal orbital.

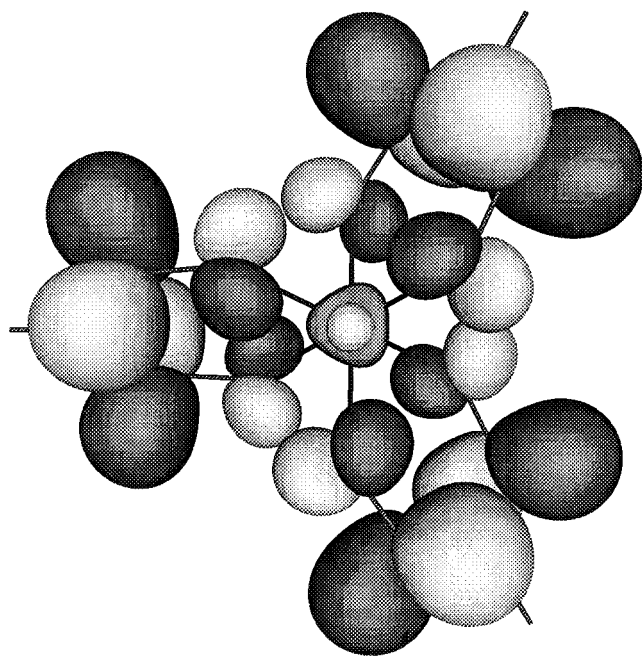


Figure 4. Contour plot of the lowest unoccupied ligand χ type orbital of a_1 symmetry. The metal orbital in the center is the $a_1(t_{2g})$ component.

π -conjugation. In Figure 3 we show the contour plot of an e combination of the ligand HOMO. Ligand orbital coupling is in-phase (ψ) and there is a bonding interaction with an $e(t_{2g})$ component on the metal center. Figure 4 shows the a_1 combination of the ligand LUMO. Here ligand coupling is out-of-phase (χ) and there is clear evidence for a π -acceptor interaction with the $a_1(t_{2g})$ component on the metal. The extent of ligand-to-metal delocalization is not very pronounced, as could be expected of moderate π -bonding.

The calculations do not support the alternative hypothesis that

the trigonal splitting might originate from misdirected valency.³⁰ Note that Atanasov and Schönher^{3,4} already dismissed this hypothesis on the basis of its inability to predict the correct sign for $\Delta(t_{2g})$.

In the calculations of the ZFS of the 4A_2 ground-state we observed a sizable anisotropy in the spin-orbit coupling with the excited states $^2T_{1g}$ and $^4T_{1g}$. The source of this anisotropy can be traced mainly to two effects.³¹ McGarvey has for different Cr(III) compounds investigated the effect of configurational interaction on the ZFS of the ground state.^{25,32} He concluded³² that a very small distortion of the charge distribution, compressing the trigonal axis, was sufficient to induce anisotropy in the spin-orbit coupling. The other mechanism is that of covalent anisotropy introduced by Stevens and Owen^{33,34} to explain some features of the optical spectrum in transition metal complexes. Examples of recent applications to highly covalent transition metal complexes can be found in refs 35 and 36. As covalent bonds are formed between metal and ligand the metal d orbitals get diluted and as a result the spin-orbit coupling decreases. This mechanism was invoked previously by Atanasov and Schönher⁴ to explain the large ZFS in the Cr(acac)₃ complex.

The orbitals we used for the spin-orbit coupling calculation were optimized for the 2A_2 excited state and are therefore biased toward this state. To find out the reduction factors of the spin-orbit coupling from the free ion value we performed orthogonal transformations³⁷ on the d orbitals of e -type (in D_3) so that the angular parts became close to octahedral form with the e_g and the t_{2g} shell separated. With simultaneous O_h and D_3 symmetry adaption the angular momentum operator within the d shell has a simple form. In this way we could determine effective parallel and perpendicular spin-orbit components:³¹ $\xi_{||} = 251 \text{ cm}^{-1}$ and $\xi_{\perp} = 254 \text{ cm}^{-1}$. There is a total reduction of about 11% compared to the free ion value $\xi = 285 \text{ cm}^{-1}$ but no pronounced anisotropy.

We conclude therefore that orbital mixing between the t_{2g} and the e_g shells is the source of the anisotropy of the spin-orbit coupling matrix elements between the 4A_2 ground state and the E and A components of the 4T and 2T states. This mixing is induced by the trigonal field of the ligands. The first orbital in Figure 3 is occupied and describes some of the excess negative charge on the PDO ligand that resides in the delocalized π -orbital. Clearly we see that a substantial fraction of the charge is located in the backbone and this indeed points toward a component of the ligand field with a trigonal compression. This coincides with the conclusion of McGarvey²⁵ for the Cr(acac)₃ complex.

5. Conclusions

We have performed ab initio calculations on Cr(PDO)₃ in an attempt to clarify some pending controversies concerning the

- (30) Bridgeman, A. J.; Gerloch, M. The interpretation of ligand field parameters. In *Progress in Inorganic Chemistry*; Karlin, K. D., Ed.; John Wiley & Sons, Inc.: New York, 1997; Vol. 45, p 179.
- (31) Ceulemans, A. *Top. Curr. Chem.* **1994**, 171, 27.
- (32) McGarvey, B. R. *J. Chem. Phys.* **1964**, 40, 809.
- (33) Stevens, K. W. H. *Proc. R. Soc. (London)* **1953**, 219, 542.
- (34) Owen, J. *Proc. R. Soc. (London)* **1955**, 227, 183.
- (35) Deaton, J. C.; Gebhard, M. S.; Solomon, E. I. *Inorg. Chem.* **1989**, 28, 877.
- (36) Gebhard, M. S.; Deaton, J. C.; Koch, S. A.; Millar, M.; Solomon, E. I. *J. Am. Chem. Soc.* **1990**, 112, 2217.
- (37) Under any orthogonal transformation within the active space, the restricted full CI wave function and energies are invariant. This means that we can apply orthogonal orbital rotations of the type $\psi'_1 = \psi_1 \cos(\alpha) - \psi_2 \sin(\alpha)$, $\psi'_2 = \psi_1 \sin(\alpha) + \psi_2 \cos(\alpha)$ to any pair of orbitals ψ_1, ψ_2 in the active space.

nature of the ligand field transitions in the closely related $\text{Cr}(\text{acac})_3$. Three important conclusions could be reached.

(i) A significant trigonal splitting of the ${}^4\text{T}_{2g}$ parent state is reproduced with the correct sign for a perfectly octahedral first coordination sphere. The shape of the molecular orbitals indicates the presence of a phase-coupling effect from the unsaturated chelating bridge.

(ii) The unusually large ZFS of the ground state could be reproduced as well and can indeed be traced to an anisotropic spin-orbit mechanism. The source of this anisotropy is clearly identified as orbital mixing between the t_{2g} and the e_g shells. Due to the delocalized nature of the π -electrons we expect backflow of electrons from oxygen and a trigonal compression component of the ligand field.

(iii) The absolute positions of the doublet states were overestimated by about 2500 cm^{-1} . The spin-orbit coupled emitting doublet state is predicted to be $2\bar{\text{A}}({}^3/2)({}^2\text{E}_g)$, which is in agreement with spectral assignment but in conflict with excited-state EPR experiments. The large ZFS of the ${}^2\text{E}_g$ level cannot be reproduced and may be based on a wrong assignment.

Acknowledgment. This investigation has been supported by grants from the Flemish Science Foundation (FWO), the Concerted Action of the Flemish Government, and by the European Commission through the TMR program (Grant ERBF-MRXCT960079). We thank Dr. T. Schönher for a print out of the absorption spectra of $\text{Al}(\text{acac})_3:\text{Cr}^{3+}$, reported in ref 6.

IC980161S